Pattern-Reconfigurable Mobile Terminal Antenna System for MIMO and Link Stabilization in LTE

Syrytsin, Igor A.; Vestager, Henrik A.; Nørgaard, Søren B.; Thomsen, Lasse; Barrio, Samantha Caporal Del; Pedersen, Gert F.

Published in:
12th European Conference on Antennas and Propagation (EuCAP 2018)

DOI (link to publication from Publisher):
10.1049/cp.2018.0892

Publication date:
2018

Document Version
Accepted author manuscript, peer reviewed version

Citation for published version (APA):
Syrytsin, I. A., Vestager, H. A., Nørgaard, S. B., Thomsen, L., Barrio, S. C. D., & Pedersen, G. F. (2018). Pattern-Reconfigurable Mobile Terminal Antenna System for MIMO and Link Stabilization in LTE. In *12th European Conference on Antennas and Propagation (EuCAP 2018)* Institution of Engineering and Technology (IET). https://doi.org/10.1049/cp.2018.0892

Pattern-Reconfigurable Mobile Terminal Antenna System for MIMO and Link Stabilization in LTE

Igor Syrytsin *, Henrik A. Vesterager, Søren B. Nørgaard, Lasse Thomsen, Samantha Caporal Del Barrio *, Gert F. Pedersen *

* Department of Electronic Systems, Aalborg University, Aalborg, Denmark, {igs, scdb, gfp}@es.aau.dk

***Abstract*—In this paper, a pattern reconfigurable mobile phone antenna system for enhanced data rates in the LTE communication scheme is proposed. The three driven antennas are designed with a resonant frequency of 2.6 GHz (Band VII). Passive elements are utilized in the design in order to change the radiation pattern direction of the proposed antennas. The designed antennas are primarily made to obtain pattern reconfigurability in data mode, where the phone is held either vertically with one hand or horizontally with two hands. Seven different radiation pattern directions are achieved with the proposed antenna setup. With the use of RF switches and tuning devices, such as a programmable array of capacitors (PACs), this architecture can be implemented in handheld terminals. In this work, prototypes with fixed architecture and different lengths of passive elements are presented. Finally, the MIMO performance of the system is investigated by calculating the envelope correlation coefficients, which are under 0.25 in the band of interest.**

***Index Terms*—Mobile antenna, pattern reconfigurable, IFA, slot, data mode, passive elements.**

I. Introduction

The performance of high-speed data transfer on mobile devices has become a very important aspect of our everyday life, as streaming movies, loading images, and browsing web pages on mobile devices has increased with the smartphone revolution. There are multiple subsystems, antennas, and protocols, which can be optimized for better data rates, however, this paper focuses on the antennas used in phones and specifically the radiation pattern and losses due to the harsh stochastic nature of the environment where mobile devices are required to work, be it on a moving train or in the basement of a concrete building in a large city. In such environments where there is no direct line of sight (nLOS) to the base-station, the received radio waves will often be a combination of multiple waves coming from different directions which have been split due to multipath, diffraction, and reflections. This phenomenon can cause a shadowing effect, where there are some areas within a room that suffers from very little coverage [1]. By using pattern reconfigurable antennas (PRA), the radiation beam can be pointed towards the area with the most signal coverage for link optimization. Besides recovering from shadowed regions, such as user's hands or head, the PRA's can also lower the body losses and increase MIMO performance. Especially in data mode, where the mobile device is either held vertically with one hand or horizontally with two hands, the hands are covering most of the phone. The desired vertical and horizontal radiation pattern modes are displayed in Fig. 1. It has been shown that the body loss is a large factor for handheld terminals [2], [3]. In this case, where the phone is used in data mode, the primary body loss comes from the hand. Furthermore, the antenna performance of newer smartphones is often worse compared to older models. It has been measured that the total radiated power in the GSM bands has decreased by 7 dB from earlier models to today's models [4]. This also imposes that the antenna design needs more attention in order to improve the overall throughput. The communication distance can be doubled at 2.6 GHz for a link improvement of 10 dB if the typical values for LTE [5] and an extended COST model [6] are used.

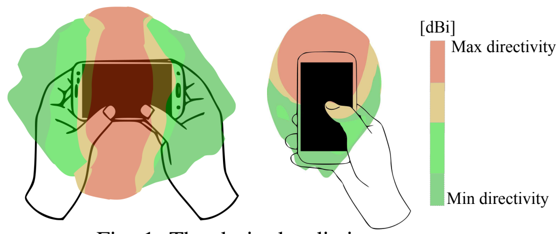

Fig. 1. The desired radiation patterns.

PRA can be built in several ways, such as using more than one antenna, mechanical changes in structure geometry, or use of passive elements such as directors and reflectors [7]. The antenna presented in this paper is a combination. It consists of three antennas with associated passive elements for rough and fine grain switching capabilities. Previously designed PRAs with parasitic elements have been researched in other papers [8], [9] designed for ISM band and 3.65 GHz respectively. In [10] a pattern reconfigurable MIMO antenna with an operating frequency reconfigurable from 4 to 14 GHz has been presented for the application of mobile terminals. In [11] a high gain pattern reconfigurable MIMO antenna array has been presented for the frequency of 5 GHz. However, no pattern reconfigurable 3x3 MIMO antennas at LTE bands have been presented yet.

This work focuses on the pattern reconfigurable antennas for the cellular mobile terminal application. The antennas are designed to comply with the LTE band VII specification. The specifications of this LTE band dictate a bandwidth of 200 MHz centered around 2.6 GHz [5]. In this work, two Inverted-F (IFA) antennas have been mounted on the short edge of the ground plane and a slot has been etched in the middle of the ground plane. Simulations including a simplified display model have shown that the slot antenna also works in a realistic environment. Passive wire elements have been used in order to change radiation pattern direction of the antennas. A directivity of up to 8 dBi has been achieved. Furthermore, the envelope correlation coefficient (ECC) of the antennas in different configurations has been calculated. An ECC of below 0.25 has been achieved in band VII. Finally, the simulations have been verified by measurements in a Satimo StarLab chamber. Good agreement between measurements and simulations has been achieved.

II. Methodology and Antenna Design

In this section the antenna system design procedure is explained. In order to achieve the desired radiation directions shown in Fig. 1 three antennas has been constructed. The desired directions of the radiation patterns are chosen such so the shadowing effect of the hands is minimal. The antennas are simulated using the transient solver in the CST Microwave Studio and the measurements are done using Satimo StarLab. All antennas are designed with a ground plane (GP) of 120 mm $\times$ 50 mm and FR4 substrate with 1.6 mm thickness. The size of the GP is comparable to that of a typical modern smartphone.

The proposed antenna design is shown in Fig. 2 along with dimensions of the antenna elements in three planes. As it is seen here, the design is based on three antennas: One slot antenna and two Inverted-F Antennas (IFA). Around the antennas are a number of switchable passive elements (PE).

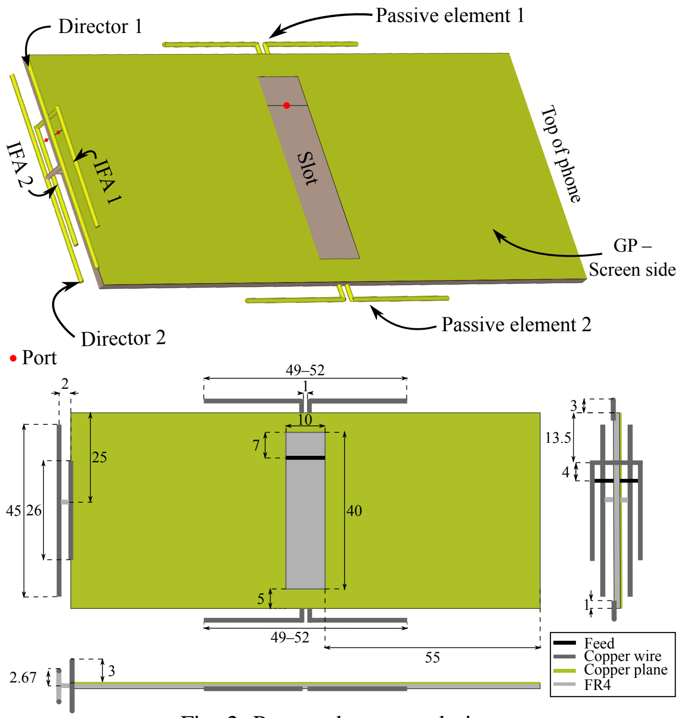

Fig. 2. Proposed antenna design.

The slot antenna is designed to have three changeable pattern-modes, corresponding to a beam going right, left, and downwards from the middle of the phone. These modes are designed for horizontal use as illustrated in Fig. 3 as M1, M2, and M3 respectively. The passive elements have been strategically placed in the location where the strongest surface currents are present. To find the optimum length of the passive elements, initial calculations were based on [12], from which it is stated that the length of a director can be calculated as 0.45λ. In the reflector case, the passive elements were made 5 % longer than the driven element. From the initial lengths, a parametric sweep was made in CST Studio to fine tune the lengths. It was found that optimum length of each arm of the passive element is 24 mm to be a director and 25.5 mm to be a reflector. The element can be changed from reflector to director by changing the electrical length of an element with a tunable capacitor.

The IFAs are designed to have four changeable pattern-modes, corresponding to a beam in the back-top, front-top, back-bottom, and front-bottom directions. These modes are intended for the vertical use of the phone as illustrated in Fig. 3 as M4, M5, M6, and M7, respectively. The IFAs make use of two directors placed outside the GP. This means that the directors should be built into the case of the phone itself. In application, the two directors could be separately controlled by switching them to ground. In the measurements of fixed prototypes, the length was varied by changing the physical length of each PE. In the simulation, a simple lumped element has been used as a loss-less switch. When the PE is floating, the IFA is able to strongly couple and the PE becomes the main radiating element which in this case radiates towards the bottom of the phone as shown in Fig. 3.

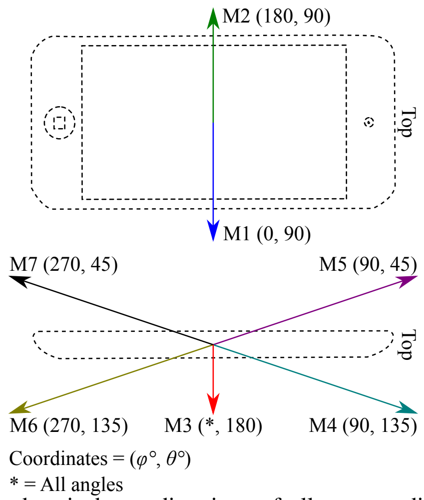

Fig. 3. Desired main beam directions of all seven radiation pattern modes. Each operating mode is color coded.

Described above are the fine-grain radiation pattern modes. These are the pattern modes for each of the antennas. The rough-grain pattern-mode, i.e, the switching between the slot antenna and the IFAs could be achieved using an absorptive FET-based switch. The cost of this, however, is added loss. The proposed switching circuit is shown in Fig. 4. Two switches are used for switching between antennas (S1, S2), two are used for connecting the two PEs for the IFAs (S3, S4), one for shorting the slot antenna at the middle when the IFAs are active (S5), and two variable capacitors for electrically varying the length of the slot antenna's PEs, making them function as either directors or reflectors (C_1, C_2). The switch and capacitor configurations for the different radiation pattern modes are shown in Table I.

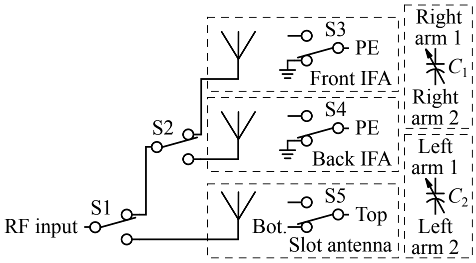

Fig. 4. Switching circuit and PE control. The two IFA directors can be grounded or open. The electrical length of the slot's left and right PEs are varied with variable capacitors. The slot can be shorted at the middle when the IFAs are active.

	M1	M2	M3	M4	M5	M6	M7
S1	Slot	Slot	Slot	IFA	IFA	IFA	IFA
S2	–	–	–	Back	Front	Back	Front
S3	Open	Open	Open	Gnd	Gnd	Gnd	Open
S4	Open	Open	Open	Gnd	Gnd	Open	Gnd
S5	Open	Open	Open	Closed	Closed	Closed	Closed
C_1	LowC	HighC	HighC	–	–	–	–
C_2	HighC	LowC	HighC	–	–	–	–

Tab. I. Switch and capacitor configurations for different radiation pattern modes.

A. *Simulation with Display and Hands*

From [13] it is known that the effects of hands causes detuning and absorption losses. To show the concept of pattern reconfigurability for a mobile device in data mode, the antennas have been simulated with two hands in the positions proposed in Fig.1. From the simulations with the one and two hands in data mode, it is concluded that around −3.5 dB of absorption loss is introduced. Simultaneously, the hands detune the antenna reflection coefficient, increasing the total loss even more. It can be concluded that it is possible to obtain around 50 % efficiency in an antenna when the body loss from the user's hands is taken into account. This only applies if the resonant frequency is tuned to 2.6 GHz.

Simulations have also been carried out with a screen, i.e. a sheet of Perfect Electrical Conductor (PEC), hovering the board and connected to the GP. The simulations showed that the slot antenna was only influenced in the direction of the screen radiation, where the screen acts as a large reflector. However, the radiation patterns from the sides, M1 and M2, are still present. This shows that the proposed antenna system can potentially be implemented in an actual modern smartphone.

B. *Prototype and Measurement Setup*

Four antenna prototypes have been made in total, however, three of those are similar slot antenna prototypes with different lengths of passive elements. The prototypes of the slot and IFA systems are shown in Fig. 6. The slot antenna has been matched by an air-wound inductor yielding a high Q-value. Here it is also seen that the slot antenna is shorted across the middle to avoid coupling when the IFAs are measured. One prototype was built for the two IFAs in Fig. 6. The antennas are fed using separate SMA connectors. To change between the different modes, the PEs are grounded systematically during measurements and the unused SMA connector is terminated to 50 Ω, to illustrate the absorptive switch behavior. The IFAs are matched to 2.6 GHz using a variable capacitor which is also shown in Fig. 6. The antennas have been measured in a Satimo chamber as shown in Fig. 5. The position of the prototypes is chosen such that the highest accuracy and spatial sampling rate are achieved. However, after post-processing, the radiation patterns have been rotated in order to have the same coordinate system in both setups.

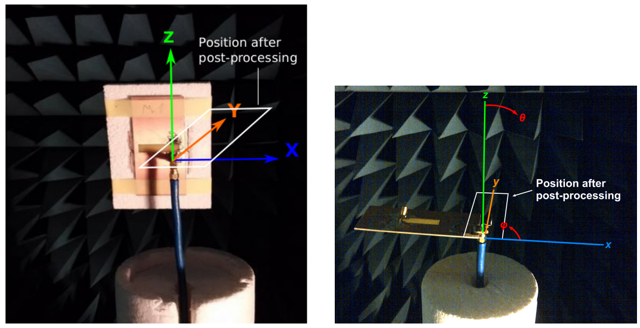

(a) (b)

Fig. 5. Measurement setup (a) when slot antenna is measured and (b) when IFA antennas are measured

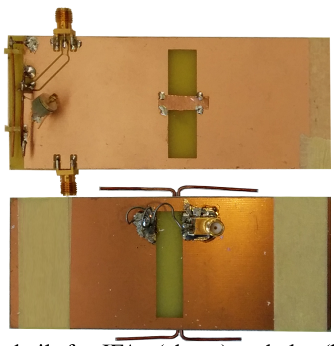

Fig. 6. Prototypes built for IFAs (above) and slot (below). Note that the lengths of the PEs shown by the slot antenna are for radiation pattern mode M1 (reflector above, director below).

III. Measurement Results

In this section the measured and simulated results are presented.

A. *Radiation Patterns*

The resulting three radiation patterns for the slot antenna and the four radiation patterns for the two IFA antennas are shown in Fig. 7 and 8, respectively. These results are based on the prototypes described in Section II-B. The figures show the radiation patterns in three planes: *xy*, *zy*, and the *zx*. The mobile phone with respect to each plane is illustrated by the orange outline along with comments about the orientation of the phone around the polar plots. It is seen that the simulated

Pattern Mode	D_0 [dBi] S	D_0 [dBi] M	ϕ [°] D	ϕ [°] S	ϕ [°] M	θ [°] D	θ [°] S	θ [°] M
M1	8.0	5.6	0	5	10	90	95	70
M2	6.8	7.0	180	185	185	90	95	128
M3	3.3	3.3	*	270	287	180	45	126
M4	6.2	4.5	90	95	91	135	124	125
M5	4.1	3.2	90	90	81	45	50	54
M6	3.4	3.1	270	244	267	135	155	149
M7	3.5	5.6	270	260	268	45	25	50

Tab. II. Maximum directivity of the simulated (S) and measured (M) antenna pattern modes compared with the desired (D) pattern directions in Fig. 3.

Pattern mode	f_r [GHz] S	f_r [GHz] M	BW [GHz] S	BW [GHz] M	Efficiency [%] M_m	Efficiency [%] M_p
M1	2.66	2.60	2.57–2.74	2.40–2.79	52	63
M2	2.68	2.64	2.69–2.83	2.37–2.77	38	78
M3	2.63	2.54	2.57–2.74	2.30–2.86	56	73
M4	2.77	2.58	2.69–2.89	2.41–3.00+	33	75
M5	2.66	2.58	—	2.54–2.74	16	88
M6	2.35	2.54	2.22–2.51	2.30–2.66	39	63
M7	2.60	2.59	2.53–2.67	2.49–2.69	41	77

Tab. III. Simulated (S) and measured (M) antenna parameters. Here, f_r is the resonant frequency, BW is the −6 dB bandwidth, and Efficiency in the minimum measured efficiency within 2.5–2.7 GHz (M_m) and the measured peak efficiency (M_p).

and measured patterns share similarities but are not exactly identical. This is, however, to be expected due to the placement of cables and connectors, etc. The main beam directions and maximum directivity for each mode are presented in Table II. The table includes the simulated, measured, and desired results of the PRA. These results share the same characteristics as those of the radiation pattern plots.

Next, the bandwidth, efficiency, and resonant frequency for each pattern-mode can be found in Table III for both simulated and measured results. Here it is seen that the frequency is shifted down when the passive elements are activated. This has the unfortunate effect of detuning the resonant frequency, which yields in the lower total efficiency. This is why, in some cases, the measured efficiency is lower than anticipated. The bandwidth of the antennas suffering from low efficiency and below the requirements for LTE band VII, however, most of these issues could be solved by better matching with components.

B. MIMO Performance

The potential of the proposed reconfigurable antenna array system to be used in a 3×3 MIMO system has been investigated in this subsection by simulations. If the proposed system should work as MIMO then the switching circuit will be different than the one shown in Fig. 4. Usually the MIMO performance of an antenna is characterized by the isolation between antennas and the envelope correlation coefficient (ECC). The measured and simulated isolation between the antennas is lower than −10 dB, which is acceptable for mobile antennas. The ECC is shown in Fig. 9(a) for different radiation pattern mode combinations. Notice that the slot antenna cannot operate at the same time as the IFAs when the radiation pattern mode 4 and 5 are used. The ECC between the IFAs and the slot antenna is high when the radiation pattern modes 4 and 5 are

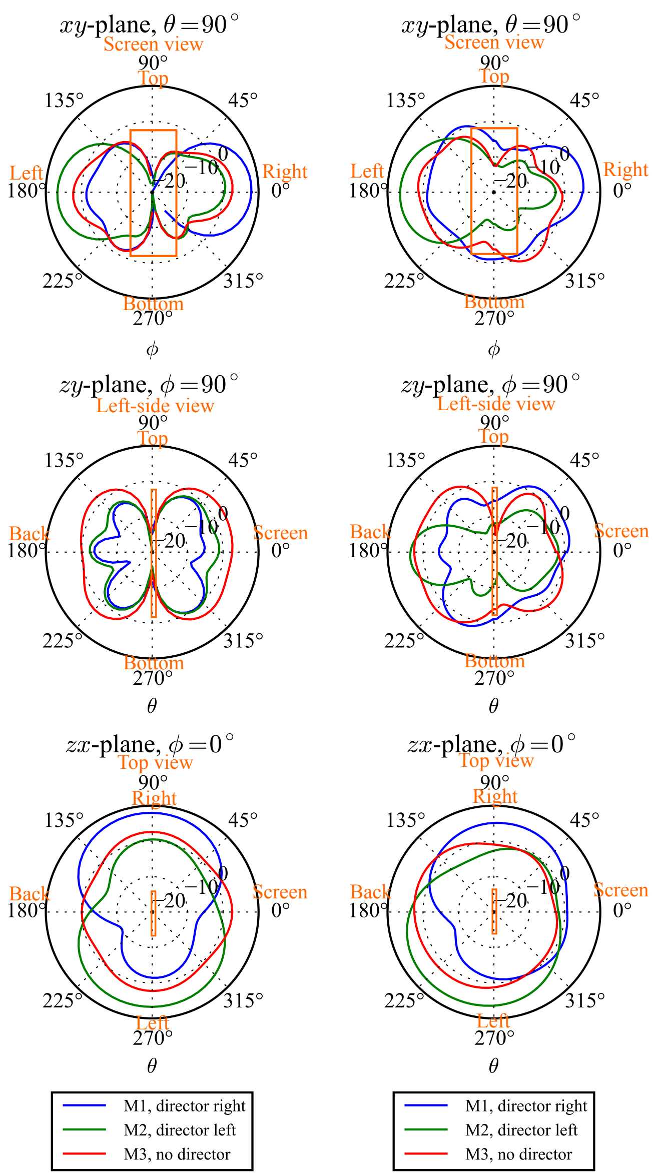

(a) Simulated. (b) Measured.

Fig. 7. Simulated and measured radiation patterns of the slots pattern modes.

used. This due to the IFAs' radiation pattern pointing towards the slot antenna. Otherwise, the ECC is under 0.25, which will mean that MIMO performance of the antenna system will be reasonable. Finally, the diversity gain of the antenna system in different configurations has been presented in Fig. 9(b). An omnidirectional channel has been used for calculation, because of the rich multi-path at 2.6 GHz and arbitrary mobile terminal orientation, as the user can hold a mobile terminal in many different ways. From the results, it can also be seen that a gain of 8.7 dB or higher has been achieved in the band of interest.

IV. Conclusion

This paper has presented a method of achieving pattern reconfigurability in handheld terminals that complies with the LTE Band VII. The presented antenna system allows for rough

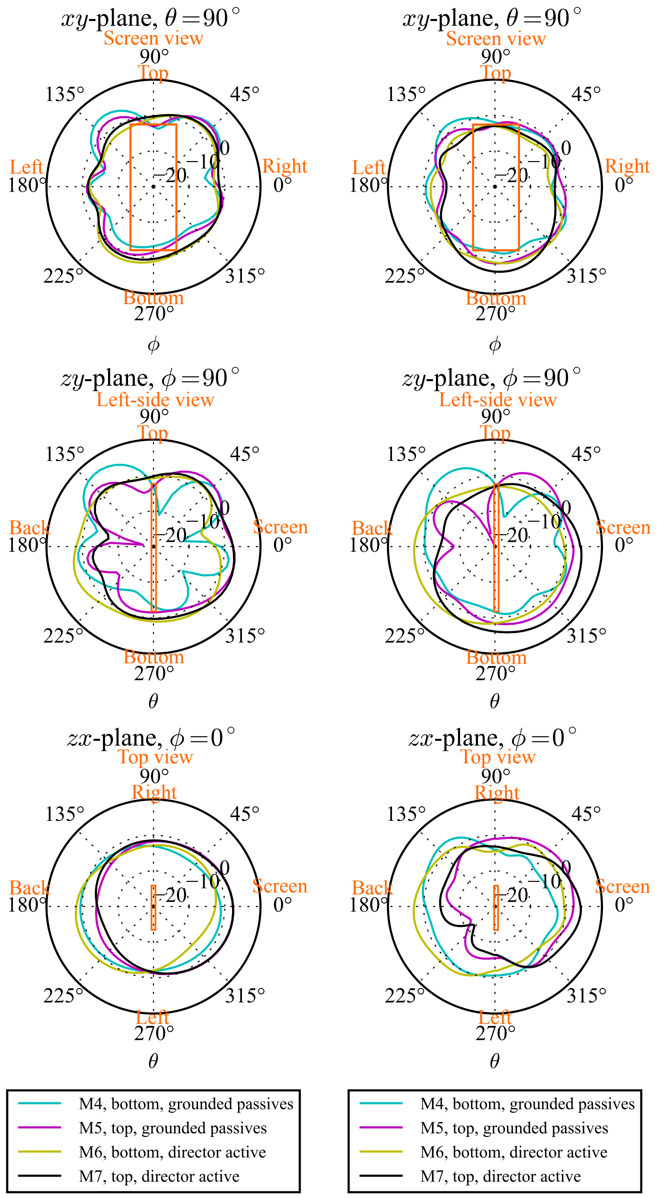

(a) Simulated. (b) Measured.

Fig. 8. Simulated and measured radiation patterns of the IFAs pattern modes.

and fine grain pattern tuning through a combination of three antennas and four passive elements. The design is based on two IFAs and one slot antenna. The beam can be switched in 7 different directions with a maximum directivity of up to 8 dBi. It is noticed that the resonance frequency lowers when the antenna is loaded with passive elements. However, this could be fixed by counter matching the antennas at the feed with capacitors and inductors. Next, antenna system prototypes have been constructed and measured in a Satimo chamber. High similarity between measurements and simulations have been achieved. Furthermore, the antenna system 3×3 MIMO performance has been verified by calculating the ECC between the different radiation pattern modes.

In application, it should be possible to tune the antennas

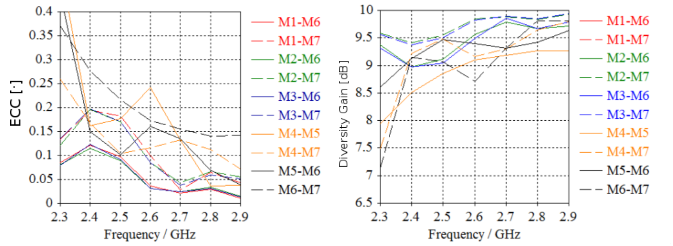

(a) (b)

Fig. 9. MIMO performance metrics: (a) envelope correlation coefficient and (b) diversity gain between the radiation pattern modes of the antenna system.

using a programmable array of capacitors by counteracting the detuning before the antennas are loaded with the passive elements. This detuning results in a lower total efficiency at the measured resonant frequency and therefore some of the antennas are not able to meet the requirement of a minimum efficiency of 50 % in the 200 MHz band. However, measured peak efficiency is higher than 60 % in all of the antenna system configurations.

REFERENCES

[1] J. S. Seybold, *Introduction to RF Propagation*. Wiley-Interscience, 2005-09-20.

[2] A. Tatomirescu and G. F. Pedersen, "Body-loss for popular thin smart phones," 2013.

[3] J. Krogerus, J. Toivanen, C. Icheln, and P. Vainikainen, "User effect on total radiated power and 3-d radiation pattern of mobile handsets," 2006.

[4] A. Morris, S. Barrio, J. Shin, V. Steel, and G. Pedersen, *Tunable Antennas for Mobile Devices: Achieving High Performance in Compelling Form Factors*. I E E E - M T T S International Microwave Symposium. Digest, IEEE Press, 2014.

[5] H. Holma and A. Toskala, *LTE for UMTS: Evolution to LTE-Advanced*. Wiley, 2011.

[6] "REPORT ITU-R SM.2028-1 Monte Carlo simulation methodology for the use in sharing and compatibility studies between different radio services or systems." White Paper, 2002.

[7] J. T. Bernhard, *Reconfigurable Antennas*. Morgan and Claypool, 2007.

[8] I. B. Trad, J. M. Floc'h, H. Rmili, M. Drissi, and F. Choubani, "Design of reconfigurable radiation pattern dipole antenna with director and reflector elements for telecommunication systems," *Loughborough Antennas & Propagation Conference*, November 2013.

[9] S. Zhang, G. H. Huff, J. Feng, and J. T. Bernhard, "A pattern reconfigurable microstrip parasitic array," *Ieee Transactions On Antennas And Propagation, Vol. 52, No. 10*, OCTOBER 2004.

[10] S. Padmanathan, A. A. Al-Hadi, P. J. Soh, and M. F. Jamlos, "Dual port mimo half-shaped cubical parasitic pifa design for pattern and frequency reconfiguration applied in mobile terminals," in *2016 IEEE Asia-Pacific Conference on Applied Electromagnetics (APACE)*, pp. 136–140, Dec 2016.

[11] N. H. Chamok, M. H. Yılmaz, H. Arslan, and M. Ali, "High-gain pattern reconfigurable mimo antenna array for wireless handheld terminals," *IEEE Transactions on Antennas and Propagation*, vol. 64, pp. 4306–4315, Oct 2016.

[12] C. A. Balanis, *Antenna Theory Analysis And Design*. John Wiley & Sons, 2005.

[13] P. Bahramzy and G. Pedersen, "Head and hand detuning effect study of narrow-band against wide-band mobile phone antennas," *Electronics Letters*, vol. 50, no. 15, pp. 1040–1042, 2014.